The Journal of
Eukaryotic Microbiology

Published by the International Society of Protistologists

Journal of Eukaryotic Microbiology ISSN 1066-5234

ORIGINAL ARTICLE

Discovery of a Diverse Clade of Gregarine Apicomplexans (Apicomplexa: Eugregarinorida) from Pacific Eunicid and Onuphid Polychaetes, Including Descriptions of *Paralecudina* n. gen., *Trichotokara japonica* n. sp., and *T. eunicae* n. sp.

Sonja Rueckert[a,b], Kevin C. Wakeman[c] & Brian S. Leander[c]

a School of Life, Sport and Social Sciences, Edinburgh Napier University, Sighthill Campus, Sighthill Court, Edinburgh EH11 4BN, United Kingdom
b Shimoda Marine Research Center, University of Tsukuba, 5-10-1, Shimoda, Shizuoka 415-0025, Japan
c Department of Zoology, University of British Columbia, #3529–6270 University Boulevard, Vancouver, BC V6T 1Z4, Canada

Keywords
Eugregarines; parasite; phylogeny; taxonomy.

Correspondence
S. Rueckert, School of Life, Sport and Social Sciences, Edinburgh Napier University, Sighthill Campus, Sighthill Court, Edinburgh EH11 4BN, United Kingdom
Telephone number: +44 131 455 2490;
FAX number: +44 131 455 2291;
e-mail: s.rueckert@napier.ac.uk

Received: 15 June 2012; revised 13 August 2012; accepted September 25, 2012.

doi:10.1111/jeu.12015

ABSTRACT

Marine gregarines are poorly understood apicomplexan parasites with large trophozoites that inhabit the body cavities of marine invertebrates. Two novel species of gregarines were discovered in polychaete hosts collected in Canada and Japan. The trophozoites of *Trichotokara japonica* n. sp. were oval to rhomboidal shaped, and covered with longitudinal epicytic folds with a density of six to eight folds/micron. The nucleus was situated in the middle of the cell, and the mucron was elongated and covered with hair-like projections; antler-like projections also extended from the anterior tip of the mucron. The distinctively large trophozoites of *Trichotokara eunicae* n. sp. lacked an elongated mucron and had a tadpole-like cell shape consisting of a bulbous anterior region and a tapered tail-like posterior region. The cell surface was covered with longitudinal epicytic folds with a density of three to five folds/micron. Small subunit (SSU) rDNA sequences of both species were very divergent and formed a strongly supported clade with the recently described species *Trichotokara nothriae* and an environmental sequence (AB275074). This phylogenetic context combined with the morphological features of *T. eunicae* n. sp. required us to amend the description for *Trichotokara*. The sister clade to the *Trichotokara* clade consisted of environmental sequences and *Lecudina polymorpha*, which also possesses densely packed epicyctic folds (3–5 folds/micron) and a prominently elongated mucron. This improved morphological and molecular phylogenetic context justified the establishment of *Paralecudina* (ex. *Lecudina*) *polymorpha* n. gen. et comb.

GREGARINES are unicellular parasites of terrestrial, freshwater, and marine invertebrates that infect the digestive tract, coelomic spaces, and reproductive vesicles of their hosts. The vast majority of described gregarine species belong to so-called "eugregarines" (Grassé 1953; Leander 2008; Perkins et al. 2002), which possess an extracellular feeding stage, the trophozoite, that are conspicuously different in morphology and motility from the infective sporozoite stage. Most eugregarines possess dense arrays of longitudinal epicytic folds facilitating surface mediated nutrition (Leander 2008). Because of the large number of folds, the cells are relatively stiff and move using an actin/myosin-based gliding mechanism (Heintzelman 2004; Leander 2008). The trophozoites of eugregarines are also either septate or aseptate depending on whether or not the cell is partitioned into two visible compartments (protomerite and deutomerite). The anterior end of the trophozoites is modified for attachment to host tissues and is considered an epimerite in septate species and a mucron in aspetate species. Mucrons and epimerites can range from being streamlined and inconspicuous to prominent and elongated, sometimes bearing multiple hair-like extensions.

The haploid life histories of eugregarines apparently lack an asexual proliferation phase called "merogony", whereby the trophozoites are able to divide into many genetically identical individuals (Levine 1977). In general, eugregarines have (monoxenous) life cycles involving only

one host species. The relatively large trophozoites within a host pair up in a process called "syzygy" and become gamonts. A cyst forms around the pair of gamonts, forming a gametocyst, and each gamont divides into numerous gametes (Levine 1977). The pair-wise fusion of gametes derived from each gamont forms a zygote that is then surrounded by an oocyst wall. Within the oocyst, meiosis occurs to yield four (or more, with subsequent rounds of mitosis) spindle-shaped sporozoites (Kuriyama et al. 2005). Hundreds of oocysts accumulate within each gametocyst, and are usually released via host faeces or via host death and remain in the environment until a new host ingests them. Once ingested, the sporozoites hatch from the oocysts and penetrate the host cells. The sporozoites enlarge to become trophozoites that emerge from the cell and start feeding.

Lecudina Mingazzini, 1899 (Levine, 1988) and the Lecudinidae Kamm, 1922 (26 genera) are essentially "catch-all" taxa for marine eugregarines that infect mainly polychaetes (Rueckert and Leander 2010). Emerging molecular phylogenetic data combined with ultrastructural data, however, have improved our understanding of lecudinid interrelationships (Leander 2008; Leander et al. 2003b; Rueckert and Leander 2009, 2010; Simdyanov 2009). For instance, *Difficilina* (Rueckert et al. 2010; Simdyanov 2009) and *Trichotokara* (Rueckert and Leander 2010) are recently established genera within the Lecudinidae that more accurately characterize the diversity of marine eugregarines. The combination of molecular phylogenetic data, comparative morphology, host affinity, and biogeography suggest that many more genera are warranted and that some known species of *Lecudina* need to be re-evaluated within the context of available data (compare Levine 1977, 1979; Perkins et al. 2002; Landers and Leander 2005; Rueckert and Leander 2008, 2009; Simdyanov 2009). The generation of molecular phylogenetic data from characterized gregarine species has also played a huge role in the interpretation of environmental sequences generated from PCR surveys of organismal diversity in specific habitats (e.g. Rueckert et al. 2011).

In this vein, we discovered two novel species of marine eugregarines in eunicid and onuphid polychaetes and characterized their trophozoites with light microscopy (LM), scanning electron microscopy (SEM) and small subunit (SSU) rDNA sequences. Molecular phylogenetic analyses of the new sequences enabled us to (1) determine the emerging composition of a diverse *Trichotokara* clade, (2) establish the cellular identities of nine environmental sequences collected from several different habitats, and (3) re-evaluate and revise the taxonomy of "*Lecudina*" *polymorpha* within *Paralecudina* n. gen. et comb.

MATERIALS AND METHODS

Collection and isolation of organisms

Repeated dredge hauls were conducted in the Sagami-nada Sea (34°38′43″N, 138°56′16″E) in November 2010 and February 2011 at a depth of ~ 45 m during collecting trips on the research vessel R/V Tsukuba based at the Shimoda Marine Research Center, University of Tsukuba, Shimoda, Shizuoka, Japan. Onuphid tubeworms *Nothria* cf. *otsuchiensis* (Imajima, 1986) were collected from these samples. The polychaete *Eunice valens* (Chamberlin, 1919) was collected at a depth of 7–10 m while SCUBA diving at Ogden Point (48°24′48″N, 123°23′37″W), in August 2010, in Victoria, British Columbia, Canada. The intestines of the host animals were dissected with fine-tipped forceps under a low magnification stereomicroscope (Olympus SZ61, Olympus Corp. Tokyo, Japan/Leica MZ6, Wetzlar, Germany) to extract the trophozoites of *Trichotokara japonica* n. sp. and *Trichotokara eunicae* n. sp. Gut contents containing trophozoites were examined using an inverted compound microscope (Olympus CKX31, Olympus Corp./Zeiss Axiovert 200, Carl-Zeiss, Goettingen, Germany, or Leica DM IL, Wetzlar, Germany), and individual trophozoites were isolated by micromanipulation. Before being prepared for microscopy and DNA extraction, individual trophozoites were washed three times in filtered and autoclaved seawater.

Light, scanning, and transmission electron microscopy

Differential interference contrast (DIC) light micrographs of the trophozoites of *T. japonica* n. sp. were taken using a system microscope (Olympus BX50, Olympus Corp.) connected to a digital camera (Olympus DP70, Olympus Corp.). The DIC light micrographs of the trophozoites of *T. eunicae* n. sp. were taken with a compound microscope (Zeiss Axioplan 2, Carl-Zeiss) connected to a colour digital camera (Leica DC500). Individual trophozoites of *T. japonica* n. sp. ($n = 55$) and *T. eunicae* n. sp. ($n = 60$) were prepared for scanning electron microscopy (SEM) using the OsO_4 vapour protocol described previously (Rueckert and Leander 2008, 2009). Isolated cells were deposited directly into the threaded hole of a Swinnex filter holder, containing a 5 μm polycarbonate membrane filter (Millipore Corp., Billerica, MA), that was submerged in 10 ml of seawater within a small canister (2 cm diameter and 3.5 cm tall). A piece of Whatman filter paper was mounted on the inside base of a beaker (4 cm diameter and 5 cm tall) that was slightly larger than the canister. The Whatman filter paper was saturated with 4% OsO_4 and the beaker was turned over the canister. The parasites were fixed by OsO_4 vapours for 30 min. Ten drops of 4% OsO_4 were added directly to the seawater and the parasites were fixed for an additional 30 min on ice. A 10-ml syringe filled with distilled water was screwed to the Swinnex filter holder and the entire apparatus was removed from the canister containing seawater and fixative. The parasites were washed, then dehydrated with a graded series of ethyl alcohol. Prepared specimens of *T. japonica* n. sp. were freeze-dried with t-butanol and specimens of *T. eunicae* n. sp. were critical-point dried with CO_2. Filters were mounted on stubs, sputter coated with 5 nm gold, and viewed under a scanning electron microscope (JEOL NeoScope JCM5000, JEOL Ltd., Tokyo, Japan/Hitachi S4700, Nissei Sangyo America, Ltd., Pleasanton, CA).

Fifty cells of *T. eunicae* n. sp. were manually isolated from the gut of *E. valens*, washed in filtered seawater, and placed in a 1.5-ml microfuge tube filled with 2% glutaraldehyde in seawater, and chilled on ice for 30 min. Trophozoites were postfixed with 1% OsO_4 in 0.2 M sodium cacodylate buffer (SCB) (pH 7.2) for 1 h on ice, washed three times (15 min each) with 0.2 M SCB, then dehydrated with a graded series of ethanol washes (30%, 50%, 75%, 85%, 90%, 95%, and 100%) at room temperature. The sample was placed in a 1:1 acetone/ethanol mixture for 30 min, and changed into acetone thereafter. Cells were placed in 1:1 acetone/resin (Eppen 812) two times (6 h each) at room temperature, changed into resin, and held at room temperature for 10–12 h, before being polymerized overnight at 70 °C. Ultrathin sections were cut on a diamond knife, using a Leica EM UC6 microtome (Leica). Sections were placed on formvar-coated grids, post-stained with uranyl acetate and lead acetate, and viewed under a transmission electron microscope (Hitachi H7600, Nissei Sangyo America, Ltd.). Some data were presented on a grey or black background using Adobe Photoshop 6.0 (Adobe Systems, San Jose, CA).

DNA isolation, PCR amplification, cloning, and sequencing

DNA from *T. japonica* n. sp. was extracted from two different isolates of trophozoites collected at different times. Seventeen individual trophozoites (isolate 1) and 18 individual trophozoites (isolate 2) were manually isolated from dissected hosts. DNA from *T. eunicae* n. sp. was extracted from 20 individual trophozoites after isolation from their hosts. They were washed three times in filtered and autoclaved seawater, and deposited into a 1.5-ml microfuge tube.

Genomic DNA was extracted from the cells using the MasterPure complete DNA and RNA purification Kit (EPICENTRE, Madison, WI). Small subunit rDNA sequences were PCR amplified using puReTaq Ready-to-go PCR beads (GE Healthcare, Quebec, Canada) and the following eukaryotic PCR primers for *T. japonica* n. sp.: F1 5′-GCGCTACCTGGTTGATCCTGCC-3′ and R1 5′-GATCCTTCTG CAGGTTCACCTAC-3′ (Leander et al. 2003a). The following internal primers, designed to match existing eukaryotic SSU sequences, were used for nested PCR: F2 5′-AAGTCTGGTGCCAGCAGCC-3′, F3 5′-TGCGCTACCTGG TTGATCC-3′ and R2 5′-GCCTYGCGACCATACTCC-3′. The following primer pairs were used for the amplification of the SSU rDNA of *T. eunicae* n. sp.: F4 5′ TGC GCT ACC TGG TTG ATG ATC C 3′, R1 5′ GGG CGG TGT GTA CCA RGR G 3′, F5 5′ CGG TAA TTC CAG CTC C 3′, R3 5′ GAT CCT TCT GCA GGT TCA CCT CA 3′. PCR products of *T. japonica* n. sp. corresponding to the expected size (~ 1806 bp) were gel isolated and cloned into the pSC-A-amp/kan vector using the StrataClone PCR cloning kit (Agilent Technologies, Santa Clara, CA). PCR products of *T. eunicae* n. sp. were gel isolated and cloned into the pCR 2.1 vector using the TOPO TA cloning kit (Invitrogen, Frederick, MD). Eight cloned plasmids, for each PCR product, were digested with *Eco*RI, and inserts were screened for size using gel electrophoresis. Two identical clones were sequenced with ABI Big-dye reaction mix using vector primers and internal primers oriented in both directions. The SSU rDNA sequences were identified by BLAST analysis and molecular phylogenetic analyses (GenBank Accession numbers: JX426617 *T. japonica* n. sp.; JX426618, *T. eunicae* n. sp.).

Molecular phylogenetic analysis

The two new SSU rDNA sequences from *T. japonica* n. sp. and *T. eunicae* n. sp. were incorporated into a 94-sequence alignment representing the diversity of gregarines, some other important apicomplexan groups as well as dinoflagellates (outgroup) using MacClade 4 (Maddison and Maddison 2000) and visual fine-tuning. The program PhyML (Guindon and Gascuel 2003; Guindon et al. 2005) was used to analyse the 96-sequence alignment (994 unambiguously aligned positions; gaps excluded) with maximum-likelihood (ML) using a general-time reversible (GTR) model (Posada and Crandall 1998) incorporating the fraction of invariable sites and a discrete gamma distribution with four rate categories (GTR + I + Γ + 4 model: $\alpha = 0.724$ and I = 0.193 for the 96-sequence alignment). The GTR model was selected using the program MrAIC 1.4.3 with PhyML (http://www.abc.se/~nylander/mraic/mraic.html). ML bootstrap (MLB) analyses were performed on 100 re-sampled datasets using the same program and the same GTR + I + Γ + 4 model.

We performed two additional analyses (1) including the three *Trichotokara* species, the closely related environmental sequence and two environmental sequences from the *Paralecudina* clade as an outgroup (GTR + I + Γ + 8 model: $-\ln L = 5043.79542$, $\alpha = 0.696$ and I = 0.139 for this 6-sequence alignment) and (2) including the three *Trichotokara* species, the closely related environmental sequence and two *Selenidium* species as an outgroup (GTR + I + Γ + 8 model: $-\ln L = 4245.65172$, $\alpha = 2.777$ and I = 0.438 for this 6-sequence alignment). The analyses were performed to further evaluate the relationship between the *Trichotokara* species. As the resulting phylogenies were similar to the ones from the 94-sequence alignment, the data are not presented here.

Bayesian analysis of the 94-sequence alignment was performed using the program MrBayes 3.0 (Huelsenbeck and Ronquist 2001). The program was set to operate with GTR, a gamma-distribution, and four Monte Carlo Markov chains (MCMC; default temperature = 0.2). A total of 2,000,000 generations were calculated with trees sampled every 50 generations and with a prior burn-in of 100,000 generations (2000 sampled trees were discarded; burn-in/convergence was checked manually). A majority rule consensus tree was constructed from 38,001 post-burn-in trees. Posterior probabilities (BPP) correspond to the frequency at which a given node was found in the post-burn-in trees. Independent Bayesian runs on each alignment yielded the same results.

GenBank accession numbers

(AF494059) *Adelina bambarooniae*, (FJ459737) *Amoebogregarina nigra*, (AJ415519) *Amoebophrya* sp. ex. *Prorocentrum micans*, (DQ462459) *Ascogregarina armigerei*, (DQ462456) *Ascogregarina* culicis, (DQ462455) *Ascogregarina taiwanensis*, (AY603402) *Babesia bigemina*, (HQ891113) *Cephaloidophora* cf. *communis* from *B. balanus*, (HQ876008) *Cephaloidophora* cf. *communis* from *B. glandula*, (L19068) *Cryptosporidium baileyi*, (AF093489) *Cryptosporidium parvum*, (AF093502) *Cryptosporidium serpentis*, (AF39993) *Cytauxzoon felis*, (FJ832159) *Difficilina paranemertis*, (FJ832160) *Difficilina tubulani*, (U67121) *Eimeria tenella*, (AB191437, AB252765, AB275006, AB275008, AB275074, AB275068, AB275069, AB275070, AB275071, AB275073, AB275103, AF372767, AF372768, AF372769, AF372770, AF372771, AF372779, AF372780, AF372821, AF290084,AY179975, AY179976, AY179977, AY179988, EU050982) Environmental sequences, (FJ832163) *Filipodium phascolosomae*, (FJ976721) *Ganymedes themistos*, (FJ459741) *Gregarina blattarum*, (FJ459743) *Gregarina coronata*, (FJ459746) *Gregarina kingi*, (AF129882) *Gregarina niphandrodes*, (FJ459748) *Gregarina polymorpha*, (AF022194) *Gymnodinium fuscum*, (HQ876007) *Heliospora caprellae*, (HQ891114) *Heliospora* cf. *longissima* from *E. verrucosus*, (HQ891115) *Heliospora* cf. *longissima* from *E. vittatus*, (AF286023) *Hematodinium* sp., (AF130361) *Hepatozoon catesbianae*, (FJ459750) *Hoplorhynchus acanthatholius*, (DQ093796) *Lankesteria abbotti*, (EU670240) *Lankesteria chelyosomae*, (EU670241) *Lankesteria cystodytae*, (AF080611) *Lankesterella minima*, (FJ832157) *Lecudina longissima*, (FJ832156) *Lecudina phyllochaetopteri*, (AF457128) *Lecudina tuzetae*, (FJ459753) *Leidyana haasi*, (AF457130) *Leidyana migrator*, (DQ093795) *Lithocystis* sp., (AB000912) Marine parasite from *Tridacna crocea*, (AY334568) *Mattesia geminata*, (AF457127) *Monocystis agilis*, (AJ271354) *Neospora caninum*, (AF129883) *Ophryocystis elektroscirrha*, (AY196706) *Paralecudina* (ex. *Lecudina*) *polymorpha* morphotype 1, (AY196707) *Paralecudina* (ex. *Lecudina*) *polymorpha* morphotype 2, (FJ459755) *Paraschneideria metamorphosa*, (AY196708) *Platyproteum vivax*, (FJ459756) *Prismatospora evansi*, (FJ459757) *Protomagalhaensia granulosae*, (DQ093794) *Pterospora floridiensis*, (DQ093793) *Pterospora schizosoma*, (GQ149767) *Rhytidocystis cyamus*, (DQ273988) *Rhytidocystis polygordiae*, (M64244) *Sarcocystis muris*, (JN857968) *Selenidium boccardiella*, (JN857967) *Selenidium idanthyrsae*, (JN857966) *Selenidium* cf. *mesnili*, (FJ832161) *Selenidium orientale*, (FJ832162) *Selenidium pisinnus*, (DQ683562) *Selenidium serpulae*, (AY196709) *Selenidium terebellae*, (DQ176427) *Syncystis mirabilis*, (AF013418) *Theileria parva*, (HQ876006) *Thiriotia pugettiae*, (M97703) *Toxoplasma gondii*, (JX426618) *Trichotokara eunicae* n. sp., (JX426617) *Trichotokara japonica* n. sp., (GU592817) *Trichotokara nothriae*, (JN857969) *Veloxidium leptosynaptae*

RESULTS

Morphology of *Trichotokara japonica* n. sp. (Fig. 1–11)

The trophozoites of *T. japonica* n. sp. were approximately 123 μm long (63–201 μm, $n = 12$). Trophozoites were rigid and capable of gliding motility. The trophozoites were divided into the cell body proper and an elongated mucron (Fig. 1, 7). The cell body proper was oval to slender rhomboidal measuring 98 μm in length (50–168 μm, $n = 12$) and 25 μm in width (13–42 μm, $n = 12$). From the widest point of the cell body proper, the cell was quite symmetrical. The posterior end of the cell was rounded (Fig. 1, 4, 7), while the anterior end of the cell narrowed into a neck-like structure at the base of the elongated mucron. The mucron was shorter than the cell body proper and measured 13.4 μm in length (7.5–33.0 μm, $n = 7$) and 7.1 μm in width (5.9–8.0 μm, $n = 7$). There was no septum visible at the junction between the cell body proper and the mucron (Fig. 1–3). Instead, there was another structure situated at the base of the mucron, namely a flap-like protrusion (Fig. 1, 2, 4, 5, 8–11). Some trophozoites lacked the mucron completely and there was no visible damage to the cell (Fig. 9); other trophozoites lacked the mucron, and it seemed to have broken off (Fig. 11). A spherical nucleus measured 17.2 (11.4–20.8) μm in diameter ($n = 6$) and was mostly situated in the middle of the cell body proper or slightly shifted to the anterior end (Fig. 1, 4, 5). A nucleolus that measured 10.5 μm in diameter was observed in one trophozoite. The cytoplasm had a granular appearance (Fig. 1, 2). Gamonts without elongated mucrons were observed in side-by-side intertwined syzygy (Fig. 6). Neither sporozoites nor oocysts were observed in our samples.

Scanning electron micrographs showed that the trophozoite body surface was inscribed by densely packed longitudinal epicytic folds (6–8 folds per micron) (Fig. 7). The flap-like protrusion at the base of the mucron was also covered with epicytic folds that were continuous with the rest of the cell body proper (Fig. 8, 11). Epicytic folds merged together near the posterior and anterior ends (Fig. 10). The epicytic folds on the mucron were replaced by hair-like projections with a mean length of 1.7 μm (1.3–2.4 μm, $n = 14$) and a mean width of 0.3 μm (0.25–0.34 μm, $n = 13$) (Fig. 7, 8, 10). The hair-like projections were protrusions from the underlying cortex (Fig. 10). Antler-like projections at the tip of the mucron were only visible in the scanning electron micrographs (Fig. 7, 8). The base of the antler-like projections was 1.2 (1.1–1.4) × 1.2 (1.1–1.3) μm (Fig. 8). In most cases, the antler-like projections consisted of three branches, but in one observed case, it consisted of four branches (Fig. 8). The branches were 5.7 μm (3.9–8.2 μm, $n = 14$) long and 0.6 μm (0.43–0.73 μm, $n = 12$) wide.

Morphology of *Trichotokara eunicae* n. sp. (Fig. 12–19)

The trophozoites of *T. eunicae* n. sp. were very long with an approximate length of 581 μm (531–658 μm, $n = 11$) (Fig. 12, 14). The shape of the cell was reminiscent of a tadpole with a bulbous anterior region and a slender tail-like posterior region (Fig. 12, 14, 16). There was no evidence of an elongated mucron covered in hair-like projections. Trophozoites were brown in colour due to accumulations of amylopectin in the cytoplasm. Cells were

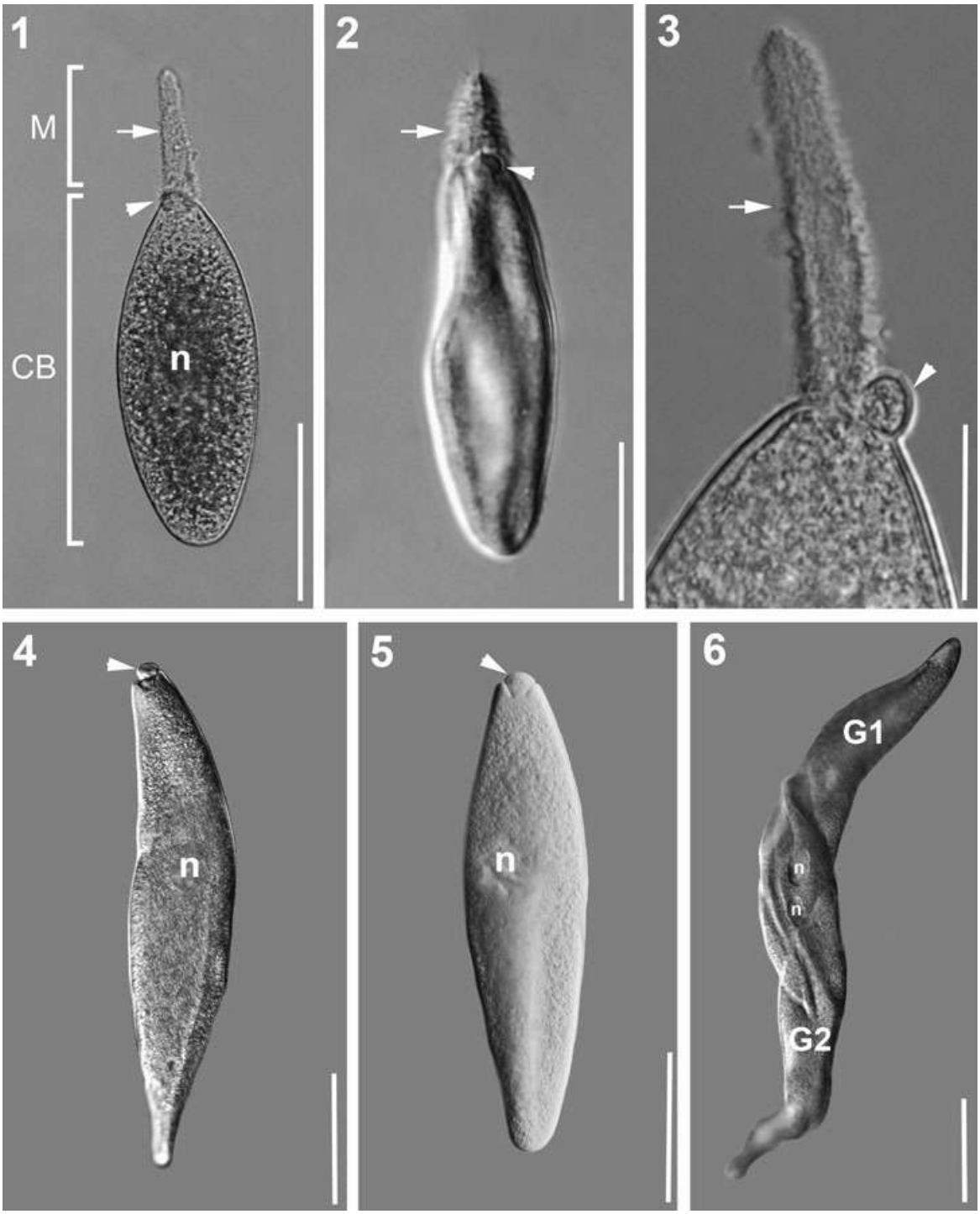

Figure 1–6. Differential interference contrast (DIC) micrographs of *Trichotokara japonica* n. sp. isolated from the onuphid polychaete *Nothria* cf. *otsuchiensis*. **1-2.** Different individual trophozoites showing morphological variability. The trophozoite can be divided into an elongated mucron (M) and the cell body proper (CB). Cell shape of the trophozoites is oval to rhomboidal with an elongated mucron (arrow). The mucron is covered with hair-like projections. At the base of the mucron sits a flap-like protrusion (arrowhead). A spherical nucleus (n) is situated in the middle. The cytoplasm is granular. **3.** Higher magnification view of the mucron with hair-like projections (arrow) and the flap-like protrusion at the base (arrowhead). **4-5.** Two trophozoites without mucrons showing flap-like protrusions at the anterior end (arrowhead). No damage to the cell is visible in these trophozoites. A spherical nucleus (n) is situated in the middle of the cell body proper slightly shifted to the anterior end. **6.** Two gamonts (G1 and G2) in lateral intertwined syzygy. The nuclei (n) of both gamonts are visible. Scale bars: Fig. 1, 4–6 = 50 μm; Fig. 2 = 20 μm; Fig. 3 = 25 μm.

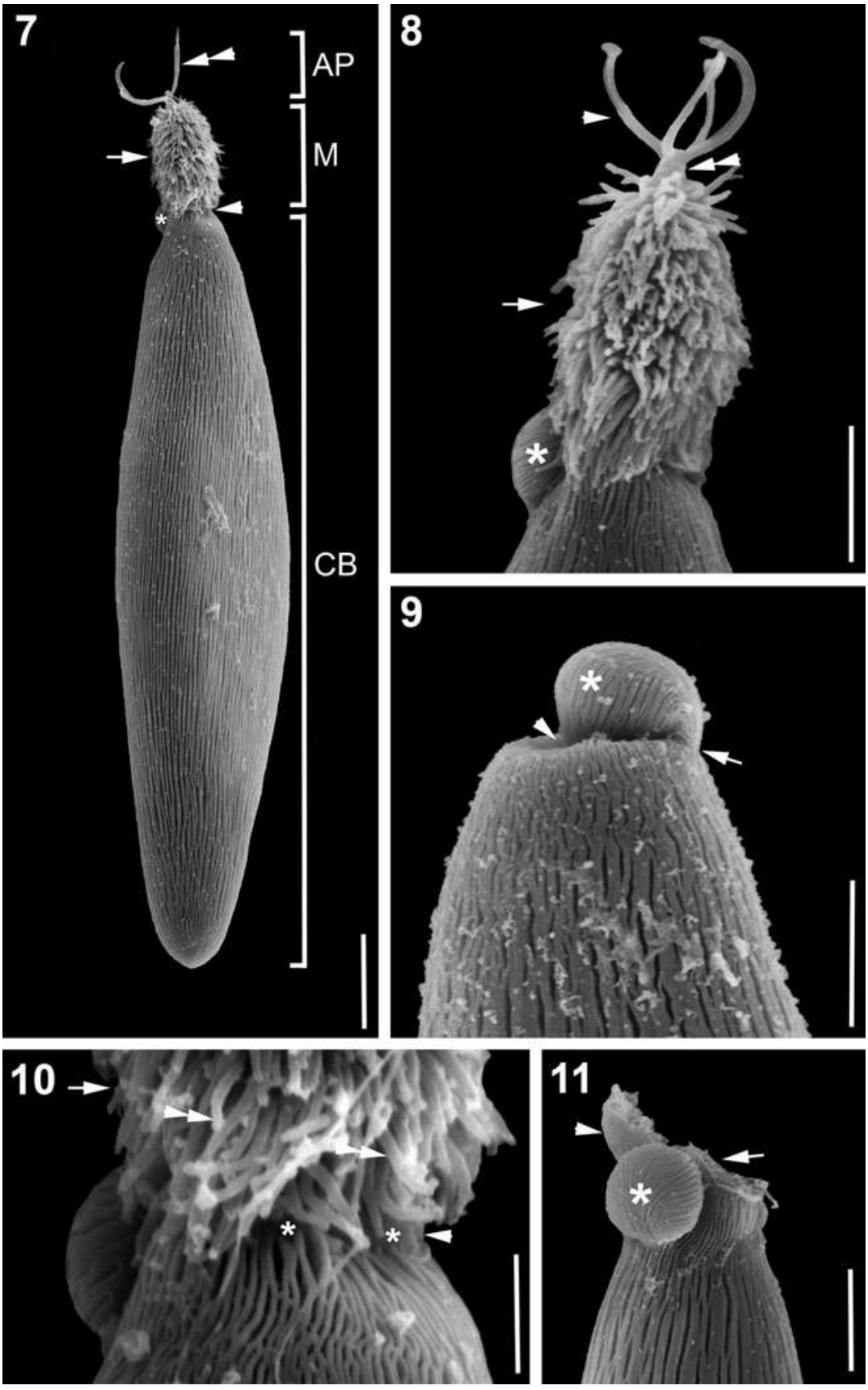

Figure 7–11. Scanning electron micrographs (SEM) showing the general morphology and surface ultrastructure of *Trichotokara japonica* n. **sp.** isolated from the onuphid polychaete *Nothria* cf. *otsuchiensis*. **7.** SEM showing a trophozoite with an elongated mucron (M) covered in hair-like projections (arrow) and an antler-like projection (AP) at the anterior tip (double arrowhead). The cell body proper is slender rhomboidal with a rounded posterior end. Densely packed longitudinal epicytic folds inscribe the cell body proper (CB). There seems to be a constriction between the mucron and the rest of the cell (arrowhead), but the vision is restricted in this micrograph. In the back of the cell at the base of the mucron lies the flap-like protrusion (asterisk). **8.** High magnification SEM of the mucron (arrow) with hair-like projections protruding from the cell surface. Situated at the anterior end of the mucron is an antler-like projection with four branches (arrowhead). The branches unite at a base that stems from the cell cortex (double arrowhead). The flap-like protrusion (asterisk) shows epicytic folds. **9.** High magnification SEM of the junction between mucron and cell body proper. There is no mucron (arrowhead) and the flap-like protrusion (asterisk) is slightly bent towards the centre, where the mucron would be otherwise. There is no cell damage visible (arrowhead). The flap-like protrusion shows epicytic folds (arrow) that are continuous with the ones on the cell body proper. **10.** High magnification SEM of the junction between the cell body proper and the elongated mucron (arrow). The epicytic folds merge together at the anterior end and stop (asterisks) at the base of the mucron (arrow) leaving a small area of smooth cortex (arrowhead) before the hair-like projections (double arrowheads) start. **11.** High magnification SEM of the junction between mucron and cell body proper. In this case there is visible cell damage (arrow) and the mucron seems to have broken off. There is still smooth cortex (arrowhead) visible on the left side of the damaged cell and the flap-like protrusion (asterisk) seems to be in its original position. Scale bars: Fig. 7 = 10 μm; Fig. 8–9, 11 = 5 μm; Fig. 10 = 2 μm.

rigid and capable of gliding motility. The broad anterior part of the cell was dorso-ventrally flattened (Fig. 16) and measured 289 μm in length (244–302 μm, $n = 11$) and 267 μm in width (254–303 μm, $n = 11$). The spherical nucleus was about 50 μm in diameter (48–53 × 47–51 μm, $n = 11$) and was situated slightly off centre in the middle of the anterior bulge (Fig. 12, 14). The bulbous anterior region was encircled by a lateral groove that was also visible along the mucron at the anterior end (Fig. 16, 17). The mucron was free of amylopectin granules and slightly protruded beyond the anterior end of the cell (Fig. 12, 13). The tail-like posterior region tapered along its length into a pointed tip with a length of 303 μm (294–317 μm, $n = 11$) and a width of 94 μm (87–106 μm, $n = 11$). There was a slight indentation at the junction between the anterior and posterior regions of the cell, but no septum was visible in either light (Inset Fig. 12) or scanning electron micrographs (Fig. 16). The entire trophozoite was covered with densely packed epicytic folds at a density of three to five folds/micron (Fig. 14, 15, 17, 18). The folds were also covered with a conspicuous layer of mucilaginous material in the form of tiny round bodies (Fig. 16, 19). Neither sporozoites, gamonts in syzygy, nor oocysts were observed in our samples.

Transmission electron microscopy showed nicely the epicytic folds of the cortex and the trilayered membrane complex (Fig. 14, 15).

Morphology of *Paralecudina polymorpha* n. gen. et comb. (ex. *Lecudina polymorpha*) (Fig. 20–22)

Two distinct morphotypes of *P. polymorpha* n. gen. et comb. (ex. *L. polymorpha*) are known from the polychaete *L. japonica* (compare Leander et al. 2003b; Rueckert et al. 2010). The cortex of both morphotypes was inscribed by numerous folds, an example of which is shown in a high magnification SEM of morphotype 1 (Fig. 20). Morphotype 1 refers to trophozoites that were 175–300 μm long and 35–50 μm wide. The anterior end was rounded with a mucron free of epicytic folds, while the posterior end was pointed. The density of folds was around three folds/micron (compare Leander et al. 2003b). Morphotype 2 refers to skinnier trophozoites that were 475–575 μm long and 35–60 μm wide with a density of folds of five folds/micron. The trophozoites of morphotype 2 often possessed a prominent bulge right behind the mucron (Fig. 21). The mucron of some trophozoites was elongated and covered in epicytic folds reaching a length of 75–100 μm and a width of 15 μm (Fig. 22). The posterior end was pointed. Both morphotypes were rigid and capable of gliding motility.

Molecular phylogenetic analyses of small subunit rDNA sequences (Fig. 23)

Phylogenetic analyses of the 96-taxon data set resulted in a strongly supported clade (90 MLB, 0.99 BPP) of dinoflagellates (outgroup) and a poorly resolved backbone for the apicomplexan ingroup (Fig. 23). The apicomplexan backbone gave rise to: (1) a clade consisting of a paraphyletic group of coccidians and a strongly supported (99 MLB, 1.00 BPP) subclade of piroplasmids; (2) a rhytidocystid clade; (3) a cryptosporidian clade; (4) a weakly supported "terrestrial gregarine clade 1" (39 MLB, 0.91 BPP), consisting of neogregarines, eugregarines from insects and an environmental sequence, as well as (5) a stronger supported "terrestrial gregarine clade 2" (20 MLB, 0.95 BPP), consisting of monocystid eugregarines and several eugregarines from insects. Two environmental sequences formed the sister clade to the two terrestrial gregarine clades. The sequences from marine archigregarines formed three different lineages (*Selenidium* species, *Veloxidium*, *Platyproteum* and *Filipodium*) that branched independently from the apicomplexan backbone (Fig. 23). Mainly marine eugregarines formed three sister clades: (1) A strongly supported clade (100 MLB, 1.00 BPP) consisting of urosporids (*Pterospora* and *Lithocystis*) and lecudinids (*Difficilina*, *Lankesteria* and *Lecudina*); (2) a strongly supported clade (100 MLB, 1.00 BPP) comprising gregarines (*Cephaloidophora*, *Ganyme-*

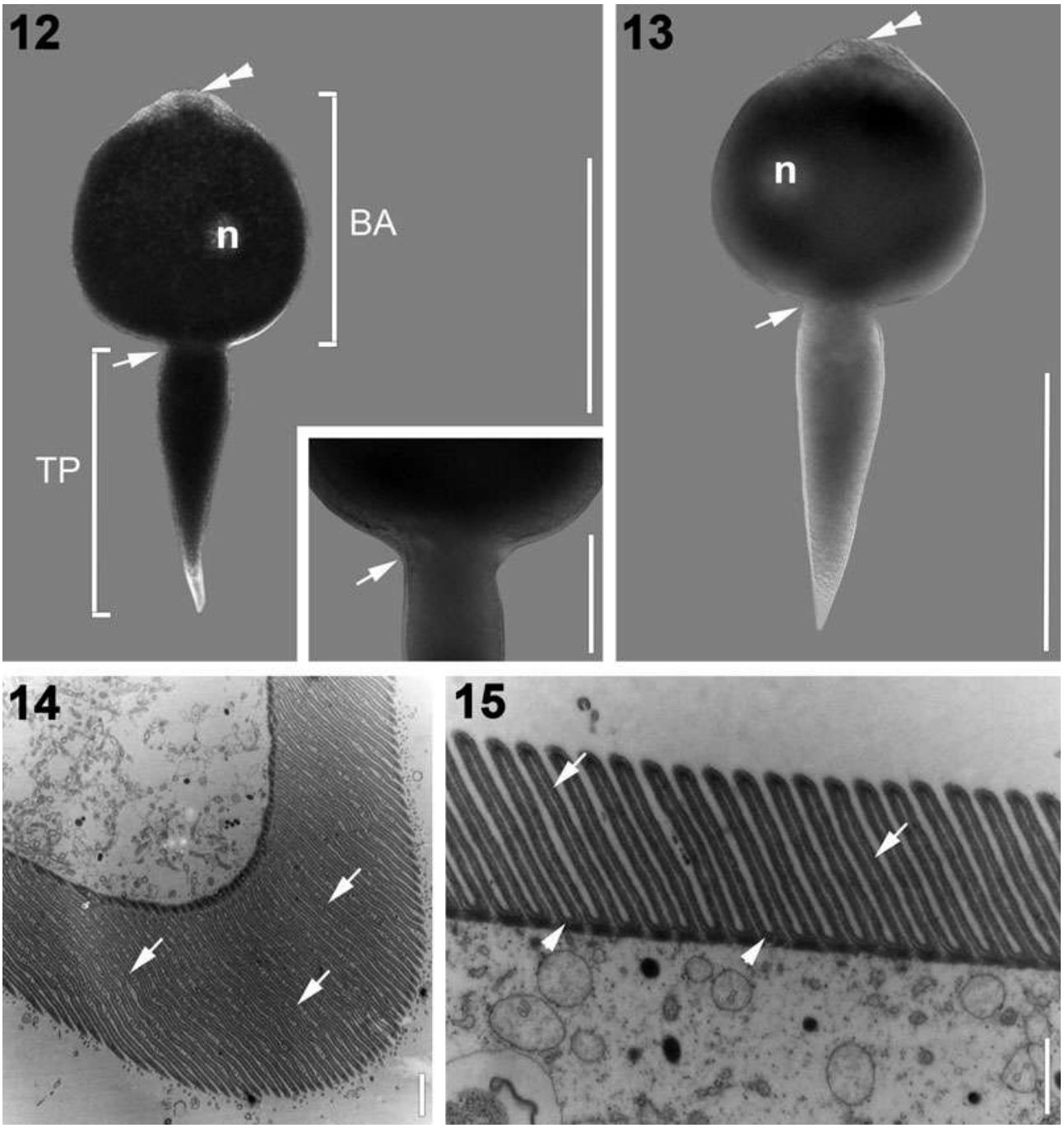

Figure 12–15. Differential interference contrast (DIC) micrographs and transmission electron micrographs (TEM) of *Trichotokara eunicae* n. sp. isolated from the eunicid polychaete *Eunice valens*. **12, 13.** Different individual trophozoites showing a slight morphological variability. The trophozoite can be divided into a bulbous anterior part (BA) and a slender tale-like posterior part (TP). Cell shape of the trophozoites is reminiscent of that of a tadpole larva. There seems to be a marginal constriction (arrow) at the junction between the anterior and posterior part of the cell. The cells are brownish in colour due to amylopectin granules in the cytoplasm. The mucron (double arrowhead) is free of amylopectin and slightly protruded. A spherical nucleus (n) is situated in the middle, slightly off centre. The inset shows a close up of the junction (arrow). There is no septum visible. **14, 15.** Transmission electron micrographs (TEM) of the cortex showing the trilayered membrane complex (arrowhead) and the epicytic folds (arrow). Scale bars: Fig. 12 = 300 μm; Inset = 75 μm; Fig. 13 = 240 μm; Fig. 14 = 2 μm, Fig. 15 = 1 μm.

des, *Heliospora* and *Thiriotia*) infesting crustaceans; and (3) a moderately supported clade (59 MLB, 0.99 BPP) consisting of *Trichotokara eunicae* n. sp., *T. japonica* n. sp., *T. nothriae*, two morphotypes of *P.* (ex. *L.*) *polymorpha* n. gen. et comb. and several environmental sequences.

Analyses of two small 6-sequence alignments (with more sites included) were performed to test the topology of the *Trichotokara* species; these analyses resulted in the same phylogenetic relationships as the analyses of the 96-sequence alignment.

A total of 1,695 bp (excluding all indels) were compared between the three species *T. nothriae*, *T. japonica* n. sp. and *T. eunicae* n. sp., by calculating the pair-wise distances based on the Kimura 2-parameter model (Kimura 1980). This resulted in a 10.1–15.3% sequence divergence between the three species. The sequence divergence between the *Trichotokara* species *T. nothriae* and *T. eunicae* was lower (10.1%) than the sequence divergence between *T. nothriae* and *T. eunicae* n. sp. (13.8%) and between *T. japonica* n. sp. and *T. eunicae* n. sp. (15.3%).

DISCUSSION

Comparative morphology

According to WoRMS (2012), the family Lecudinidae currently consists of 25 genera. Most of the described species fall within the genus *Lecudina* (Levine 1976). There are four genera within the Lecudinidae that possess hair-like projections: *Pontesia*, *Cochleomeritus*, *Diplauxis* (Levine 1977), and the recently described genus *Trichotokara* (Rueckert and Leander 2010). We described another species with this feature, namely *T. japonica* n. sp. This new species was isolated from a host (*Nothria* cf. *otsutchiensis*) that is closely related to the host of the type species of the genus, namely *T. nothriae* (*Nothria conchylega*). Both species share the features of an elongated mucron that is covered in hair-like projections and the densely packed epicytic folds, but *T. japonica* n. sp. possesses more folds per micron (6–8 folds/micron) than *T. nothriae* does (~ 5 folds/micron). The cell size and shape of the two species is different and only *T. japonica* has antler-like projections at the anterior tip of the mucron (Table 1). Projections like these have not been described before for any aseptate eugregarine species; comparable structures are only known from the epimerites of some septate (terrestrial) eugregarines (compare Perkins et al. 2002). The gamonts of *T. nothriae* undergo end-to-end syzygy (Rueckert and Leander 2010), while the gamonts of the newly described species *T. japonica* n. sp. undergo side by side intertwined syzygy. Before the gamonts undergo syzygy, they shed the mucron. Valigurová et al. (2009) discussed that in the septate gregarine species, *Gregarina polymorpha* retraction of the epimerite into the protomerite is more likely than its separation during detachment from the host epithelium. Figure 9 and 11 show both mechanisms of mucron removal. The mucron of the trophozoite in Fig. 11 broke off leaving the cell damaged. In contrast, there is no visible damage in the trophozoite shown in Fig. 9, presumably due to the retraction of the mucron.

Most gregarines within the Lecudinidae are in a size range of 100–300 μm long, with some exceptions (Perkins et al. 2002). One of the two new species we describe in this study is up to 650 μm long, namely *T. eunicae* n. sp. This gregarine, isolated from the polychaete *E. valens*, has another feature that has not been previously described: a very bulbous, dorso-laterally flattened anterior part of the trophozoite cell encircled by a lateral groove. Five gregarine species have been described from polychaetes belonging to the genus *Eunice* so far, but none for *E. valens* (compare Levine 1976, 1977). One of these species *Deuteromera cleava* Bhatia and Setna, 1938 belongs to a group of septate gregarines. The remaining four species all belong to the Lecudinidae: *Lecudina eunicae* (Lankester, 1866) Levine, 1976 from *E. harassii*; *Lecudina bhatiai* (Bhatia and Setna, 1938) Levine, 1976; *Contortiocorpa prashadi* Bhatia and Setna, 1938; and *Ulivina eunicae* Bhatia and Setna, 1938. The latter three species were isolated from *E. siciliensis*. The tadpole-like shape of the trophozoites in *T. eunicae* n. sp. differs considerably from three of the four gregarine species previously described from *Eunice* hosts. The species *L. eunicae* has a similar shape to *T. eunicae* n. sp. with a pointed wedge-shaped body posteriorly, but is significantly smaller with a length of around 254 μm (Lankester 1866). The trophozoite of *L. bathiai* is elongated oval with the widest part in the middle, narrowing at both ends (Bhatia and Setna 1938). The one character that sets *C. prashadi* apart from the other gregarines isolated from *E. siciliensisis* is that the trophozoite cell is spirally twisted upon itself (Bhatia and Setna 1938). Bhatia and Setna (1938) describe *U. eunicae* as having a neck-like protomerite with a needle-like epimerite. This contrasts greatly to the bulbous anterior region of *T. eunicae* n. sp. The trophozoite morphology of *T. eunicae* n. sp. differs significantly from the descriptions provided for all other genera and species isolated from *Eunice* hosts so far.

Molecular phylogenetic data from marine gregarines and environmental sequences

The two new sequences from the isolates described here nested within a highly supported clade consisting of *T. nothriae* and an environmental sequence (AB275074). A comparison of all three known SSU rDNA sequences (1,695 bases) resulted in a 10.1% sequence divergence between the two *T. nothriae* and *T. japonica* n. sp., a 13.8% sequence divergence between *T. eunicae* n. sp. and *T. nothriae*, and a 15.3% sequence divergence between *T. eunicae* n. sp. and *T. japonica* n. sp. These results reflect the extraordinary divergence of these sequences compared with sequences of other species in the Lecudinidae (e.g. *Lankesteria*; Rueckert and Leander 2008). The internal topology within the *Trichotokara* clade showed that the two species with trophozoites possessing an elongated mucron covered with hair-like projections, namely *T. nothriae* and *T. japonica* n. sp., are paraphyletic to a subclade consisting of environmental sequence AB275074 and *T. eunicae* n. sp. It was possible that this internal topology was an artefact associated with the very long branches for all of the sequences in this clade. Therefore, we tested this topology by analysing smaller align-

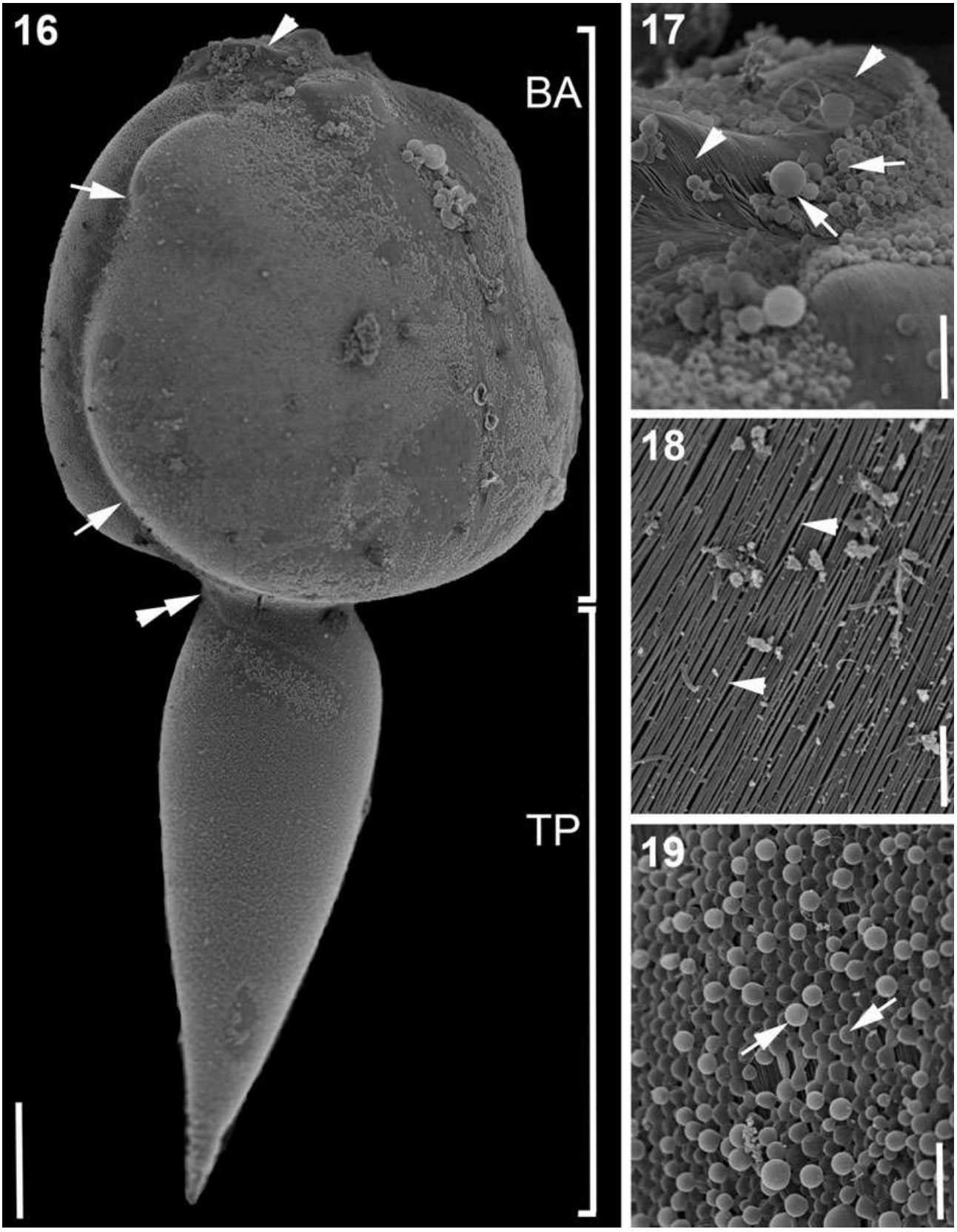

Figure 16–19. Scanning electron micrographs (SEM) showing the general morphology and surface ultrastructure of *Trichotokara eunicae* n. gen. et sp. isolated from the eunicid polychaete *Eunice valens*. **16.** SEM showing a trophozoite with a bulbous anterior part (BA) and a slender tale-like posterior part (TP) with a pointed tip. The bulbous anterior part is dorso-ventrally flattened and encircled by a lateral groove (arrows). The cell is somewhat constricted at the junction between the anterior and posterior part of the cell (double arrowhead). At the anterior tip of the cell the mucron is slightly protruded and flattened (arrowhead). **17.** High magnification SEM of the mucron area showing that even the mucron is inscribed by epicytic folds (arrowheads). Round bodies (arrows) of different size cover part of the mucron. These are most likely a type of mucilaginous material. **18.** High magnification SEM of the densely packed longitudinal epicytic folds (arrowheads). **19.** High magnification SEM of a network of generally round bodies (arrows) that covered the epicytic folds in most parts of the cell. Scale bars: Fig. 16 = 50 μm; Fig. 17 = 10 μm; Fig. 18–19 = 5 μm.

ments consisting of many more unambiguously aligned sites between the four ingroup taxa and a few outgroup taxa. The internal topology shown in Fig. 23 was consistently recovered in these analyses and suggests that trophozoites with an elongated mucron covered with hair-like projections is a synapomorphy for *Trichotokara* species that was subsequently lost in *T. eunicae* n. sp. Therefore, we chose to retain this genus name for the entire clade and amend the genus description for *Trichotokara* accordingly.

The *Trichotokara* clade also enabled us to establish the cellular identity for environmental sequence DSGM-74 (AB275074), which was previously unknown undoubtedly because of its extraordinarily long branch length (Takishita et al. 2007). This sequence was obtained from deep-sea methane cold-seep sediments (Takishita et al. 2007) and presumably stems from gametocysts or oocysts that were released from their polychaete hosts living in this environment. Environmental PCR surveys have been routinely used to approximate organismal diversity in specific habitats (Berney et al. 2004; López-Garcia et al. 2001; Stoeck et al. 2007; Takishita et al. 2007). Interpretations of these data are stifled by the absence of molecular information from many different lineages of eukaryotes (e.g. Dawson and Pace 2002; Stoeck and Epstein 2003). With regard to molecular data, marine gregarine apicomplexans are one of the most underrepresented groups of eukaryotes, and our recent findings have demonstrated that many of the environmental sequences that were interpreted as "novel kingdoms" or "early branching eukaryotes" were in fact marine gregarines (Rueckert et al. 2011). It is clear that interpretations of environmental sequences will become much more powerful as more sequences of previously undescribed gregarines become available.

The molecular phylogenetic analyses also showed that the *Trichotokara* clade forms the nearest sister group to a large clade consisting of *L. polymorpha* (also possessing trophozoites with an elongated mucron) and eight environmental sequences, albeit with moderate statistical support (59 MLB, 0.99 BPP) (Fig. 23). This more inclusive clade was very distinct from two other major clades of marine gregarines:(1) a clade consisting of *Pterospora*, *Lithocystis*, *Lankesteria*, *Difficilina, Lecudina,* and the recently described marine gregarine, *Veloxidium* and (2) a clade consisting of gregarines that infect crustacean hosts (e.g. *Cephaloidophora*, *Ganymedes*, *Heliospora*, *Thiriotia*) (Fig. 23). The phylogenetic position of *L.* cf. *tuzetae* is nested within a main marine gregarine clade that contains *Veloxidium*, a marine gregarine with morphological characteristics most similar to the archigregarine morphotype, at its base. (Wakeman and Leander 2012). However, *L.* cf. *tuzetae* has trophozoites with a basic morphology that is very similar to that of the type species of the genus *Lecudina*, namely *L. pellucida* (Leander et al. 2003b; Schrével 1969; Vivier 1968). Therefore, the molecular phylogenetic context and morphological comparisons between the trophozoites of *L. polymorpha* and *Trichotokara* demonstrate that *L. polymorpha* is clearly not a member of the genus *Lecudina*. As we alluded to in an earlier contribution (Rueckert and Leander 2010), this evidence makes it compelling to remove *L. polymorpha* from *Lecudina* and re-classify this species within a different genus. Accordingly, we have established *Paralecudina* to accommodate *P.* (ex. *Lecudina*) *polymorpha* n. gen. et comb.

Current data suggest that the molecular phylogenetic relationships of marine gregarines will become more robust and informative with the inclusion of additional sequences from newly discovered species. In this vein, it is also necessary to revisit the type species for major genera that have only been described at the morphological level, such as *L. pellucida*, to validate and modify previous inferences. Molecular phylogenetic data suggest that there are three previously unrecognized major clades of aquatic eugregarines: (1) a clade consisting of *Pterospora*, *Lithocystis*, *Lankesteria*, *Difficilina* and *Lecudina*; (2) a clade consisting of gregarines that infect crustaceans; and (3) the clade identified in this study consisting of *Trichotokara* and *Paralecudina* n. gen. We anticipate that more distinctive clades will emerge as more species of marine gregarines are characterized at the molecular level, and that the pairing of morphological and molecular data will further support our insights as we explore the diversity and evolutionary history of this unique group of marine apicomplexans.

TAXONOMIC SUMMARY

Phylum Myzozoa Cavalier-Smith and Chao, 2004
Subphylum Apicomplexa Levine, 1970
Class Conoidasida Levine, 1988
Subclass Gregarinasina Dufour, 1828
Order Eugregarinorida Léger, 1900
Family Lecudinidae Kamm, 1922
Genus *Trichotokara* amend. (Rueckert and Leander 2010) Rueckert et al. this article

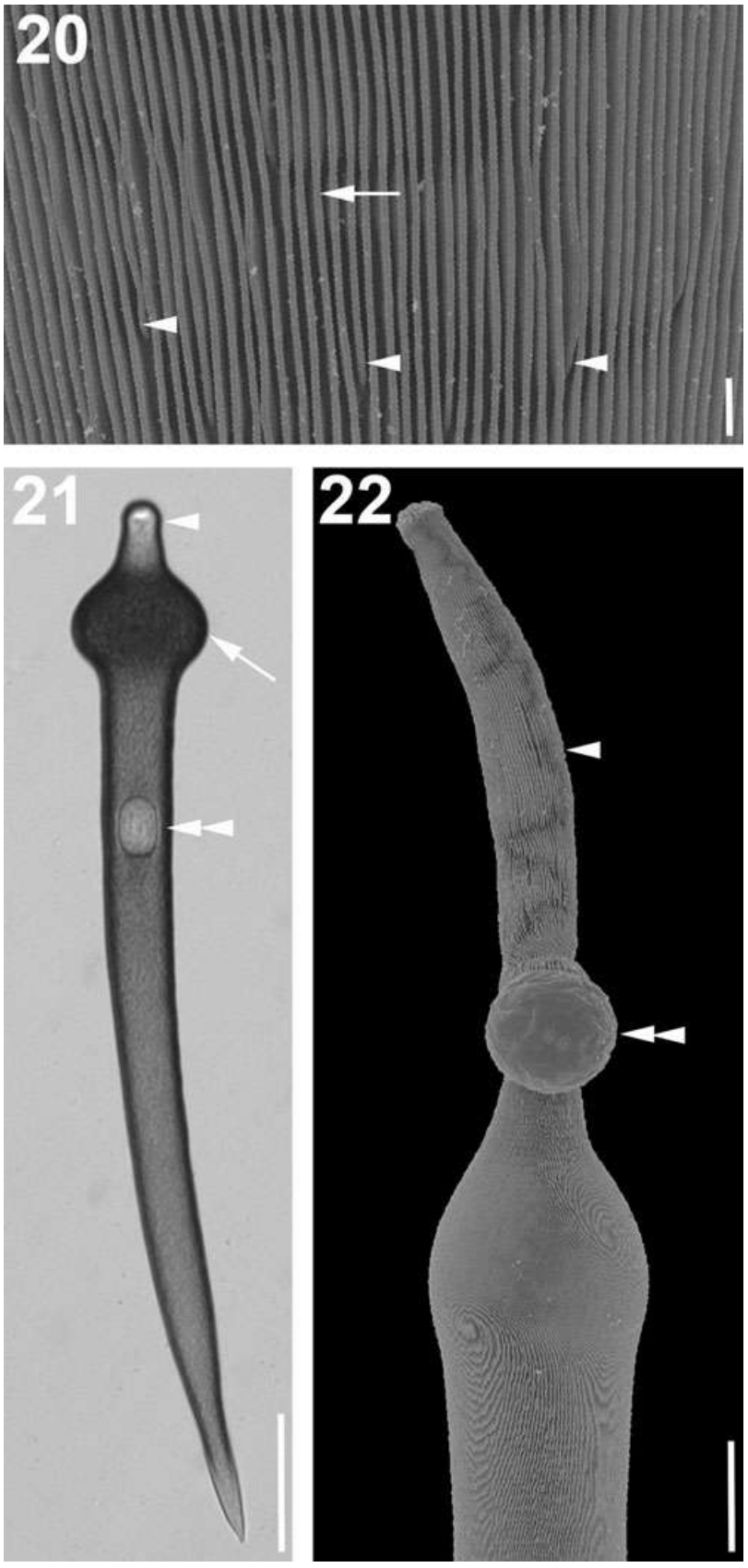

Figure 20–22. Light micrograph (LM) and scanning electron micrographs (SEM) showing general morphology and surface ultrastructure of *Paralecudina* (ex. *Lecudina*) *polymorpha* n. gen. et comb. **20.** High magnification SEM of the densely packed longitudinal epicytic folds of morphotype 1 (arrow). The arrowheads indicate terminating epicytic folds. **21.** LM of an elongated trophozoite (morphotype 2) with a pointed posterior end. The trophozoite has a prominent bulge (arrow) at the anterior end right behind the mucron (arrowhead). The oval nucleus (double arrowhead) lies in the anterior half of the cell. **22.** SEM of the elongated mucron (arrowhead) of a trophozoite (morphotype 2). The double arrowhead indicates material that was extruded from the trophozoite. Scale bars: Fig. 20 = 1 μm; Fig. 21 = 60 μm; Fig. 22 = 20 μm.

Diagnosis. Trophozoites with a dense distribution of longitudinal epicytic folds (about 5 folds/micron); mucron usually elongated and covered in hair-like projections (sometimes absent); cell body proper not or slightly dorso-ventrally flattened; posterior end rounded or tapering to a point; non-motile or gliding motility; in the intestines of eunicid and onuphid polychaetes.

Type species. *Trichotokara nothriae*

Remarks. The genus *Trichotokara* was amended to accommodate the newly described species *T. eunicae* due to the phylogenetic findings in this study. Future studies might bring evidence for a separation of this species from the genus *Trichotokara*, but at this point there are not enough reassuring data to verify this.

Trichotokara japonica n. sp. Rueckert et al. this article

Diagnosis. Trophozoites about 123 μm long (63–201 μm, $n = 12$) with an oval to slender rhomboidal shape. Cells not flattened but round in transverse section, measuring 25 μm in width (13–42 μm, $n = 12$). Cells rigid with gliding motility. Trophozoite surface inscribed by around 6–8 longitudinal epicytic folds/micron. Mucron free of folds, covered in hair-like projections that protrude from the cell surface. Posterior end of cell body rounded to pointed. Mucron 13.4 μm long (7.5–33 μm, n = 7) and 7.1 μm (5.9–8.0 μm, $n = 7$) wide, covered with hair-like projections 1.7 μm (1.3–2.4 μm, $n = 14$) long and 0.3 μm (0.25–0.34 μm, $n = 13$) wide at the base. Antler-like projections at the tip of the mucron, consisting of 3–4 branches with a length of 5.7 μm (3.9–8.2 μm, $n = 14$) and a width of 0.6 μm (0.43–0.73 μm, $n = 12$). Mucron can be absent. A flap-like protrusion situated at the base of the mucron. Spherical nucleus 17.2 (11.4–20.8) μm in diameter ($n = 6$) situated in the middle of cell body proper or slightly shifted to the anterior end. Cytoplasm granular, brownish in colour. Gamonts with side-by-side intertwined syzygy, without mucron. Neither sporozoites nor oocysts were observed.

Gene sequence. The partial SSU rDNA sequence of the gregarine, *T. japonica* has been deposited in the GenBank database under Accession number JX426617.

Type locality. Sagami-nada Sea (34°38′43″N, 138°56′16″E) near by the Shimoda Marine Research Center, University of Tsukuba, Shimoda, Shizuoka, Japan.

Type habitat. Marine; shelly gravel sediment at a depth of about 45 m.

Type host. *Nothria* cf. *otsuchiensis* Imajima, 1986 (Metazoa, Annelida, Polychaeta, Onuphidae).

Location in host. Intestinal lumen.

Holotype. Figure 7. Image taken from the holotype fixed on a gold sputter-coated SEM stub. The stub has been deposited in the Beaty Biodiversity Museum (Marine Invertebrate Collection) at the University of British Columbia, Vancouver, Canada.

Paratype. Figure 1–2

Etymology. The species name *japonica* refers to the country (Japan) where the host organisms were collected.

Remarks. The overall morphology resembles that of the previously described *Trichotokara* type species *T. nothriae*, but the possession of antler-like projections at the tip of the mucron, a flap-like protrusion at the base of the mucron, differences in size and around six to eight epicytic folds/micro, as well as the SSU rDNA sequence distinguish *T. japonica* n. sp. from *T. nothriae*.

Trichotokara eunicae n. sp. Rueckert et al. this article

Diagnosis. Trophozoites about 581 μm long (531–685 μm, $n = 11$) with a bulbous anterior region and a tail-like posterior region. The bulbous anterior region is slightly dorso-ventrally flattened, 289 μm long (244–302 μm, $n = 11$) and 267 μm wide (254–303 μm, $n = 11$), and encircled by a lateral groove. The tail-like posterior region tapers to a pointed tip and is 303 μm long (294–317 μm, $n = 11$) and 94 μm wide (87–106 μm, $n = 11$). Cells rigid and motile. Trophozoite surface inscribed by 3–5 epicytic folds/micron. Mucron forms a slight protrusion at the anterior end of the cell. Spherical nucleus ~ 50 μm in diameter (48–53 × 47–51 μm, $n = 11$) situated slightly off centre in the middle of the anterior bulbous region. Cytoplasm granular, brownish in colour; granules absent in mucron.

Gene sequence. The partial SSU rDNA sequence of the gregarine, *T. eunicae* n. sp. has been deposited in the GenBank database under Accession number JX426618.

Type locality. Ogden Point (48°24′48″N, 123°23′37″W) near Victoria, Vancouver Island, Canada.

Type habitat. Marine; rocky habitat at a depth of 10 m.

Type host. *Eunice valens* (Chamberlin, 1919) (Metazoa, Annelida, Polychaeta, Eunicidae).

Location in host. Intestinal lumen.

Holotype. Figure 16. Image taken from the holotype fixed on a gold sputter-coated SEM stub. The stub has been deposited in the Beaty Biodiversity Museum (Marine Invertebrate Collection) at the University of British Columbia, Vancouver, Canada.

Paratype. Figure 12–13

Etymology. The species name *eunicae* refers to the genus of the polychaete type host *Eunice valens* (Chamberlin, 1919).

Remarks. The phylogenetic position and the dense rows of longitudinal folds of the trophozoites places this species in the genus *Trichotokara*. The absence of an elongated, hairy mucron; differences in the size and shape of the trophozoites; and the SSU rDNA sequence distin-

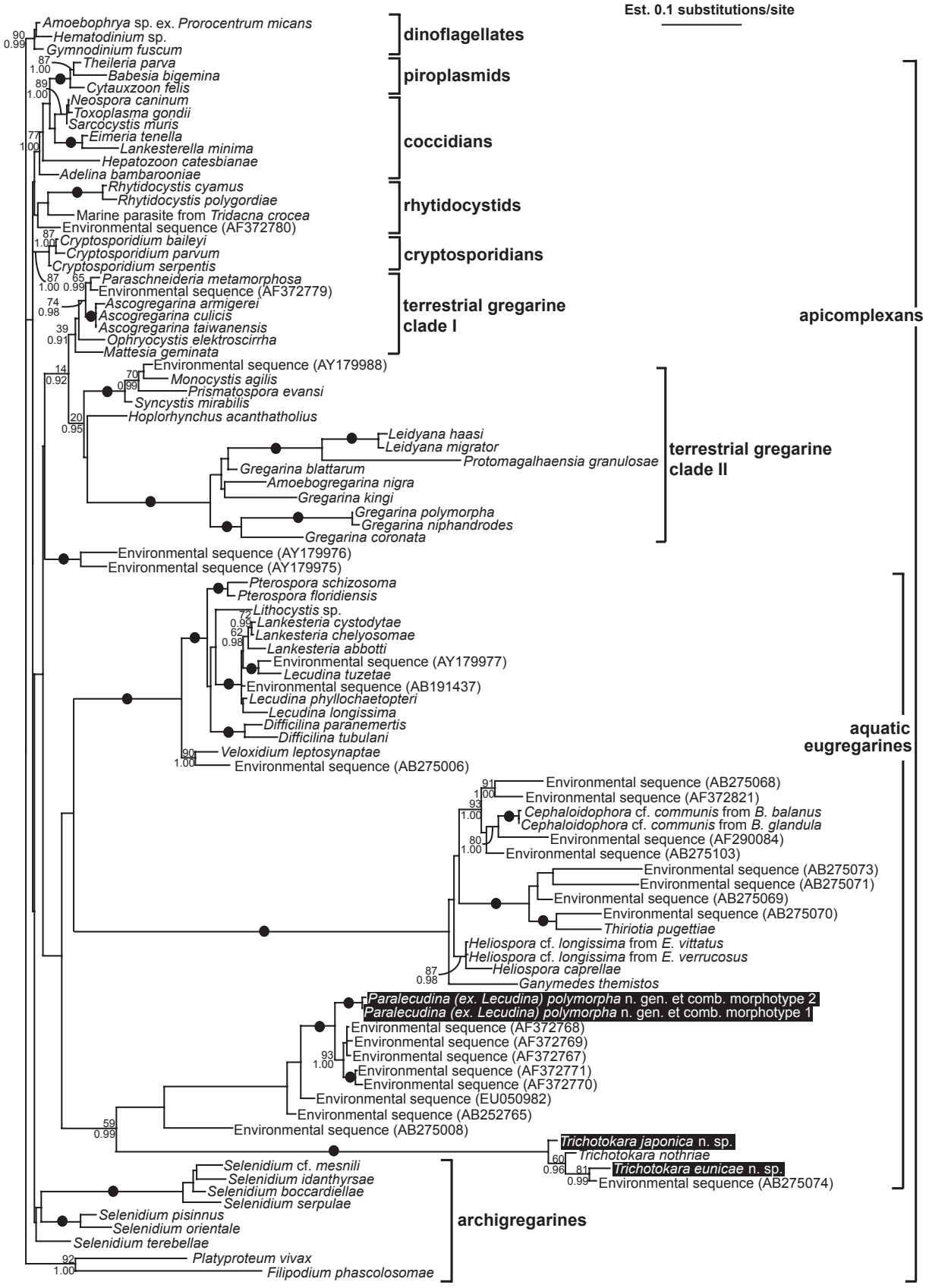

Figure 23. Maximum-likelihood tree of apicomplexans and dinoflagellates (outgroup) as inferred using the GTR model of nucleotide substitutions, a gamma-distribution and invariable sites on an alignment of 96 SSU rDNA sequences and 994 unambiguously aligned sites (−ln L = 19682.90607, α = 0.724, fraction of invariable sites = 0.193, four rate categories). Numbers at the branches denote maximum likelihood (ML) bootstrap percentages (top) and Bayesian posterior probabilities (bottom). Black dots on branches denote Bayesian posterior probabilities of 0.95 or higher and ML bootstrap percentages of 95% or higher. The sequences addressed in this study are highlighted in the black box.

Table 1. Comparison of morphological characteristics observed in *Trichotokara* species.

	Trichotokara nothriae	*Trichotokara japonica* n. sp.	*Trichotokara eunicae* n. sp.
Host	*Nothria conchylega*	*Nothria* cf. *otsuchiensis*	*Eunice valens*
Trophozoite morphology	Cell round in transverse section, not flattened	Cell round in transverse section, not flattened	Anterior part slightly dorso-ventrally flattened, posterior part round in transverse section
Cell shape	Bulges at anterior and posterior end due to constriction in the middle of the cell body	Oval to slender rhomboidal	Tadpole-like with a broad anterior end and a tail-like posterior end
Length	Cell 50–150 μm long	Cell 63–201 μm long	Cell 531–685 μm long
Width	Cell 14–55 μm wide at the widest part	Cell 13–42 μm wide at the widest part	Cell 254–303 μm wide at the widest part
Longitudinal folds	~ 5 folds/micron	6–8 folds/micron	3–5 folds/micron
Anterior end	Distinct neck-like region at anterior end	Distinct neck-like region at anterior end Flap-like protrusion at the base of the mucron	No neck-like region at anterior end
Posterior end	Rounded	Rounded	Pointed tip
Nucleus position	Nucleus in the middle of the cell body or slightly posterior	Nucleus in the middle of cell body or slightly anterior	Nucleus slightly off centre in the middle of anterior bulbous part of cell body
Nucleus size	8–20 μm in diameter	11–21 μm in diameter	~ 50 μm in diameter
Mucron morphology	Cylindrical	Cylindrical to cone shaped	Slight protrusion at anterior end
Length	14–60 μm long	8–33 μm long	
Width	6–12 μm wide	6–8 μm wide	
Appearance	Hair-like projections covering the entire length of the mucron	Hair-like projections covering the length of the mucron apart from area at the base Antler-like projection with 3–4 branches at the anterior tip of mucron	

guish *Trichotokara eunicae* n. sp. from *T. japonica* n. sp. and *T. nothriae*.

Phylum Myzozoa Cavalier-Smith and Chao, 2004
Subphylum Apicomplexa Levine, 1970
Class Conoidasida Levine, 1988
Subclass Gregarinasina Dufour, 1828
Order Eugregarinorida Léger, 1900
Family Lecudinidae Kamm, 1922
Genus *Paralecudina* n. gen. Rueckert et al. this article

Diagnosis. Trophozoites with a dense distribution of longitudinal epicytic folds (3–5 folds/micron); distinct elongation of mucron present in some morphotypes; mucron with epicytic folds; gliding motility; in the intestines of polychaetes.

Type species. *Paralecudina polymorpha* n. comb. (basionym *L. polymorpha* Schrével, 1963)

Etymology. The generic name *Paralecudina* stems from the former genus name *Lecudina* and the greek word *para*, which means beside or near. The name refers to the close morphological resemblance of the two genera.

Remarks. The new genus is established for the formerly described gregarine *L. polymorpha* Schrével, 1963 found in the intestine of *L. latreilli* and *L. japonica*. The phylogenetic position, the highly divergent SSU rDNA sequence (AY196706, AY196707), and the distinctiveness of the mucron in this lineage justify the establishment of the new genus.

ACKNOWLEDGMENTS

The authors thank the crew of R/V Tsukuba from the Shimoda Marine Research Center, University of Tsukuba for their help in collecting the specimens of *Nothria* cf. *otsuchiensis,* and Peter Lamont (SAMS, Oban, Scotland, U.K.) for his identification. This work was supported by grants from the Tula Foundation (Centre for Microbial Diversity and Evolution), the National Science and Engineering Research Council of Canada (NSERC 283091-09), the Canadian Institute for Advanced Research, Program in Integrated Microbial Biodiversity and the University of Tsukuba, Japan.

LITERATURE CITED

Berney, C., Fahrni, J. & Pawlowski, J. 2004. How many novel eukaryotic 'kingdoms'? Pitfalls and limitations of environmental DNA surveys. *BMC Biol.*, 2:13.

Bhatia, B. L. & Setna, S. B. 1938. On some gregarine parasites from certain polychaete worms from the Andaman Islands. *Proc. Indian Acad. Sci.*, 8B:231–242.

Dawson, S. C. & Pace, N. R. 2002. Novel kingdom-level eukaryotic diversity in anoxic environments. *Proc. Natl. Acad. Sci. USA*, 99:8324–8329.

Grassé, P.-P. 1953. Classe des grégarinomorphes (Gregarinomorpha, N. nov., Gregarinae Haeckel, 1866; gregarinidea Lankester, 1885; grégarines des auteurs). *In*: Grassé, P.-P. (ed.), Traité de Zoologie. Masson, Paris. p. 590–690.

Guindon, S. & Gascuel, O. 2003. A simple, fast, and accurate algorithm to estimate large phylogenies by maximum likelihood. *Syst. Biol.*, 52:696–704.

Guindon, S., Lethiec, F., Duroux, P. & Gascuel, O. 2005. PHYML Online-a web server for fast maximum likelihood-based phylogenetic inference. *Nucleic Acids Res.*, 1:33.

Heintzelman, M. B. 2004. Actin and myosin in *Gregarina polymorpha*. *Cell Motil. Cytoskeleton*, 58:83–95.

Huelsenbeck, J. P. & Ronquist, F. 2001. MrBayes: Bayesian inference of phylogenetic trees. *Bioinformatics*, 17:754–755.

Kimura, M. 1980. A simple method for estimating evolutionary rates of base substitutions through comparative studies of nucleotide sequences. *J. Mol. Evol.*, 16:111–120.

Kuriyama, R., Besse, C., Gèze, M., Omoto, C. K. & Schrével, J. 2005. Dynamic organization of microtubules and microtubule-organizing centers during the sexual phase of a parasitic protozoan, *Lecudina tuzetae* (Gregarine, Apicomplexa). *Cell Motil. Cytoskeleton*, 62:195–209.

Landers, S. C. & Leander, B. S. 2005. Comparative surface morphology of marine coelomic gregarines (Apicomplexa, Urosporidae): *Pterospora floridiensis* and *Pterospora schizosoma*. *J. Eukaryot. Microbiol.*, 52:23–30.

Lankester, E. R. 1866. Notes on the Gregarinida. *Trans. Am. Microsc. Soc.*, 14:23–28.

Leander, B. S. 2008. Marine gregarines - evolutionary prelude to the apicomplexan radiation? *Trends Parasitol.*, 24:60–67.

Leander, B. S., Clopton, R. E. & Keeling, P. J. 2003a. Phylogeny of gregarines (Apicomplexa) as inferred from small-subunit rDNA and beta-tubulin. *Int. J. Syst. Evol. Microbiol.*, 53:345–354.

Leander, B. S., Harper, J. T. & Keeling, P. J. 2003b. Molecular phylogeny and surface morphology of marine aseptate gregarines (Apicomplexa): *Selenidium* and *Lecudina*. *J. Parasitol.*, 89:1191–1205.

Levine, N. D. 1976. Revision and checklist of the species of the aseptate gregarine genus *Lecudina*. *Trans. Am. Microsc. Soc.*, 95:695–702.

Levine, N. D. 1977. Revision and checklist of the species (other than *Lecudina*) of the aseptate gregarine family Lecudinidae. *J. Protozool.*, 24:41–52.

Levine, N. D. 1979. New genera and higher taxa of septate gregarines (Protozoa, Apicomplexa). *J. Protozool.*, 26:532–536.

López-Garcia, P., Rodriguez-Valera, F., Pedros Alio, C. & Moreira, D. 2001. Unexpected diversity of small eukaryotes in deep-sea Antarctic plankton. *Nature*, 409:603–607.

Maddison, D. R. & Maddison, W. P. 2000. MacClade 4. Sinauer Associates, Sunderland.

Perkins, F. O., Barta, J. R., Clopton, R. E., Pierce, M. A. & Upton, S. J. 2002. Phylum Apicomplexa. *In*: Lee, J. J., Leedale, G. F. & Bradbury, P. (eds.), The Illustrated Guide to the Protozoa. Allen Press, Inc., Lawrence. p. 190–304.

Posada, D. & Crandall, K. A. 1998. MODELTEST: testing the mode l of DNA substitution. *Bioinformatics*, 14:817–818.

Rueckert, S. & Leander, B. S. 2008. Morphology and molecular phylogeny of *Haplozoon praxillellae* n. sp. (Dinoflagellata): a novel intestinal parasite of the maldanid polychaete Praxillella Pacifica Berkeley. *Eur. J. Protistol.*, 44:299–307.

Rueckert, S. & Leander, B. S. 2009. Molecular phylogeny and surface morphology of marine "archigregarines" (Apicomplexa) - *Selenidium* spp., *Filipodium phascolosomae* n. sp. and *Platyproteum* n. gen. et comb. - from North-eastern Pacific peanut worms (Sipuncula). *J. Eukaryot. Microbiol.*, 56:428–439.

Rueckert, S. & Leander, B. S. 2010. Description of *Trichotokara nothriae* n. gen. et sp. (Apicomplexa, Lecudinidae) - an intestinal gregarine of *Nothria conchylega* (Polychaeta, Onuphidae). *J. Invertebr. Pathol.*, 104:172–179.

Rueckert, S., Chantangsi, C. & Leander, B. S. 2010. Molecular systematics of marine gregarines (Apicomplexa) from North-eastern Pacific polychaetes and nemerteans, with descriptions of three new species: *Lecudina phyllochaetopteri* sp. nov., *Difficilina tubulani* sp. nov., and *Difficilina paranemertis* sp. nov. *Int. J. Syst. Evol. Microbiol.*, 60:2681–2690.

Rueckert, S., Simdyanov, T. G., Aleshin, V. V. & Leander, B. S. 2011. Identity of a divergent environmental DNA sequence clade using the phylogeny of gregarine parasites (Apicomplexa) from crustacean hosts. *PLoS ONE*, 6:e18163.

Schrével, J. 1969. Recherches sur le cycle des Lecudinidae grégarines parasites d'Annélides Polychètes. *Protistologica*, 5:561–588.

Simdyanov, T. G. 2009. *Difficilina cerebratuli* gen. n., sp. n. (Eugregarinida: Lecudinidae) - a new gregarine species from the nemertean *Cerebratulus barentsi* Bürger, 1895 (Nemertini: Cerebratulidae). *Parazitologiya*, 43:273–287.

Stoeck, T. & Epstein, S. 2003. Novel eukaryotic lineages inferred from small-subunit rRNA analyses of oxygen depleted marine environments. *Appl. Environ. Microbiol.*, 69:2657–2663.

Stoeck, T., Kasper, J., Bunge, J., Leslin, C., Ilyin, V. & Epstein, S. 2007. Protistan diversity in the Arctic: a case of paleoclimate shaping modern biodiversity? *PLoS ONE*, 8:e728.

Takishita, K., Yubuki, N., Kakizoe, N., Inagaki, Y. & Maruyama, T. 2007. Diversity of microbial eukaryotes in sediment at a deep-sea methane cold seep: surveys of ribosomal DNA libraries from raw sediment samples and two enrichment cultures. *Extremophiles*, 11:563–576.

Valigurová, A., Michalková, V. & Koudela, B. 2009. Eugregarine trophozoite detachment from the host epithelium via epimerite retraction: fiction or fact? *Int. J. Parasitol.*, 39:1235–1242.

Vivier, E. 1968. L'organisation ultrastructurale corticale de la gregarine *Lecudina pellucida*; ses rapports avec l'alimentation et la locomotion. *J. Protozool.*, 15:230–245.

Wakeman, K. C. & Leander, B. S. 2012. Molecular Phylogeny of Pacific Archigregarines (Apicomplexa), Including descriptions of *Veloxidium leptosynaptae* n. gen., n. sp., from the Sea Cucumber *Leptosynapta clarki* (Echinodermata), and two new species of *Selenidium*. *J. Eukaryot. Microbiol.*, 59:232–245.

WoRMS (2012). Lecudinidae. Accessed through: World Register of Marine Species. Available at: http://www.marinespecies.org/aphia.php?p=taxdetails&id=562693 [accessed on 25 December 2012].